The ALEPH Experiment

P. J. Dornan

Email alerting service	Receive free email alerts when new articles cite this article - sign up in the box at the top right-hand corner of the article or click **here**

The ALEPH experiment

By P. J. Dornan

*Blackett Laboratory, Imperial College of Science, Technology and Medicine,
London SW7 2BZ, U.K., and CERN, Geneva, Switzerland*

During 1989 and 1990 over 200000 decays of the Z boson were recorded in the ALEPH detector. The current performance of the detector is described and compared with the expectations from the original design goals.

1. Introduction

A LEP detector must be designed to address the known physics potential of the accelerator and be sufficiently flexible to accommodate the unexpected. This was the foundation for the design of ALEPH.

LEP provides the opportunity to make the most sensitive tests of the Standard Model of electroweak interactions which will probably ever be possible. The first requirement of the detector must therefore be to ensure it has the capability to make these precise tests of the electroweak theory.

Testing the Standard Model at LEP will take place at the following two energies.

1. *At the Z peak (LEP1 at a centre of mass energy ca.* 90 GeV). At this energy the electron and positron annihilate to form real Z bosons. This enables the Z mass, width and couplings to leptons and quarks to be determined with very high precision. Annihilations with longitudinally polarized electron and positron beams will eventually allow additional stringent tests.

2. *Above the* WW̄ *threshold (LEP2 at a centre of mass energy ca.* 190 GeV). At this energy the emphasis will be on the charged gauge boson, its mass, its couplings to fermions and the non-abelian ZWW̄ coupling. Investigation of longitudinal Ws, which result directly from the Higgs mechanism, will be possible.

The detector must therefore be designed to handle the increased complexity and energies of interactions at LEP2 as well as those at the Z peak.

2. The ALEPH detector: design philosophy

The ALEPH detector (Decamp *et al.* 1990) is shown in figure 1. It is relatively simple as a result of an important early decision to use as few different detection techniques as possible. The major demands were for a detector with very good tracking and a highly granular, homogeneous, calorimetric system covering as great a solid angle as possible. To provide excellent pattern recognition with the necessary momentum resolution for LEP2 a very large time projection chamber was chosen as the main tracking device with a large high field superconducting solenoid chosen to produce the magnetic deflection for the momentum measurement. For the calorimetric system the electromagnetic calorimeter is situated inside the coil to reduce the amount of material the particles traverse before they enter and the hadron calorimeter, outside the coil, serves as the magnetic field return yoke. Muon chambers are positioned on the outside of the hadron calorimeter. Luminosity
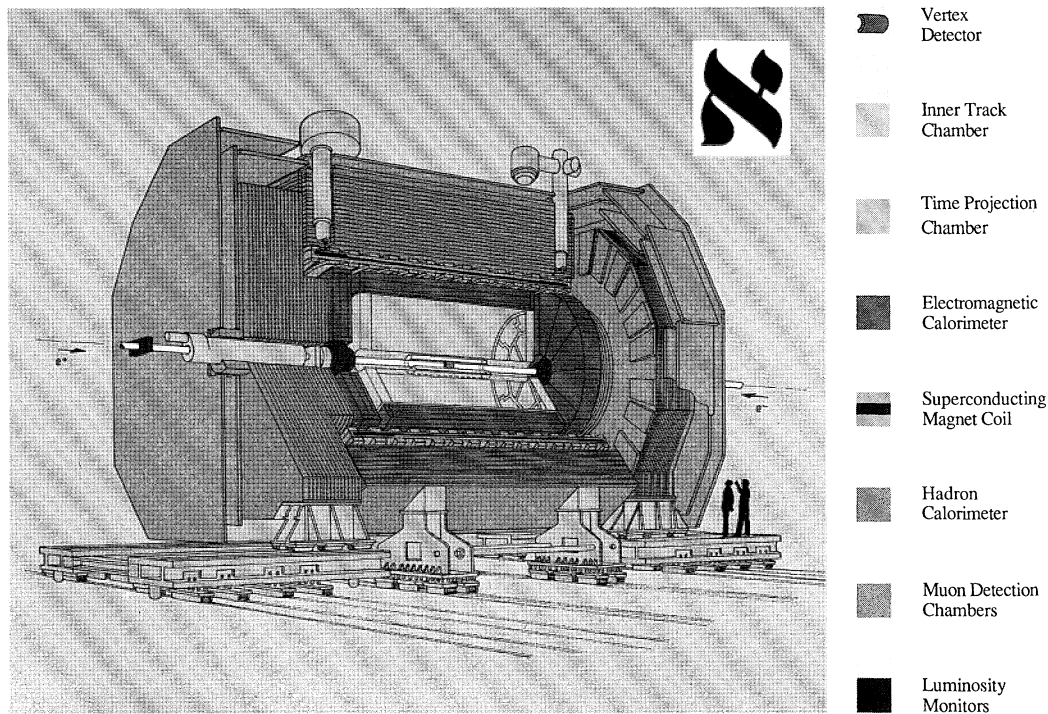
Figure 1. The ALEPH detector.

measurements are provided by tracking calorimeters situated very close to the beam line and they effectively complete the solid angle coverage of the electromagnetic calorimeter.

Both to ease maintenance and to concentrate expertise the same techniques are used in more than one place wherever possible. Hence the end caps of the calorimeters use exactly the same techniques as the barrel modules; the luminosity calorimeters the same as the electromagnetic calorimeter and the muon chambers the same streamer tubes as the hadron calorimeter. Where compromises have had to be made the emphasis for the calorimetric system has been to achieve high spatial resolution so that individual particles, particularly leptons, in jets can be identified. To maximize the solid angle coverage (hermeticity) there are as few cracks (dead regions) as possible and where they inevitably occur the calorimeters are arranged so that cracks in one are covered by the other. This makes it unlikely that any neutral particle except a neutrino or some new non-interacting object could escape without leaving a mark.

The detector is potentially capable of producing vast amounts of data following an interaction. This can take up to 4 ms to readout compared with the 22.5 µs between each crossing. As interactions occur at a rate of about 10 min^{-1} efficient trigger and data acquisition systems are required to minimize dead time. When failures do occur it is a necessity to appreciate this as soon as possible and hence clear error reporting is a prime requisite for the data acquisition. There is also very detailed online monitoring of data quality. Some errors, however, only reveal themselves when the data is fully reconstructed and so there was an early policy decision to make the full reconstruction effectively in real time at the experiment. This is accomplished with

the FALCON system which involves a number of cheap processors able to access data directly on the online computer.

A LEP detector must continue to produce precise data over a period of about eight months per year and hence sophisticated systems of monitoring and calibration must be used to correct for electronic drifts and temperature and pressure variations. Small defects at this level are not easily found even with a full reconstruction; they just contribute to a general downgrade in performance.

In the following the ALEPH tracking system and calorimetry will be described with particular emphasis on the large time projection chamber and the electromagnetic calorimeter which form the heart of the overall detector.

3. The tracking system

The tracking system has three components. From the interaction the particle trajectories are recorded first with a silicon microstrip vertex detector (MVD), then with the inner tracking chamber (ITC) and finally with the time projection chamber (TPC). The ITC is a fairly conventional wire drift chamber which provides the tracking information close to the beam and the tracking component of the event trigger. The large TPC is the most ambitious part of ALEPH. The MVD was not fully operational in 1990.

In ALEPH high momentum resolution is obtained by having a very long track length and a superconducting solenoid producing a field of 1.5 T. The large TPC and high field also aid the pattern recognition as the relative curvatures in the magnetic field cause the charged particles in the tightly collimated jets to separate. Problems can be caused by the many spiralling soft electrons but the three-dimensional nature of the points produced in the TPC enable this to be handled.

3.1. *The* ALEPH *TPC*

This is the largest detector of this type ever constructed; it is absolutely critical to the performance of ALEPH. It is a very large cylinder containing mainly noble gas which ionizes along the trajectory of a charged particle in the same way as any gaseous ionization detector. The essential difference between a TPC and more conventional chambers follows from the fact that the electric field is parallel to the magnetic field unlike the normal configuration with an azimuthal electric field and an axial magnetic one. As a result the drift volume contains only gas and ionization electrons drift parallel to the axis to proportional chambers at the endplates.

An isometric view of the ALEPH TPC is shown in figure 2. The cylinder has its axis parallel to the 1.5 T magnetic field with the electric field, produced by a 25 μm high voltage central membrane, parallel to the magnetic field in one half and anti-parallel in the other. The device is extremely large with inner and outer diameters of 0.62 m and 3.6 m and a total length of 4.4 m. Consequently the maximum drift length for the ionization electrons is 2.2 m. The TPC is intrinsically a three-dimensional device and is designed to detect coordinates along the trajectories to typically 200 μm in the $r\phi$ coordinate perpendicular to the beam axis and about 1 mm in the z coordinate along the beam direction. It is the correlation of the precise $r\phi$ and z coordinates which gives the TPC its three-dimensional imaging capability and provides the major advantage over conventional wire chambers. One price one pays for this is a very long drift distance which takes *ca.* 45 μs but this is acceptable in the LEP environment as long as the experiment has a separate trigger.
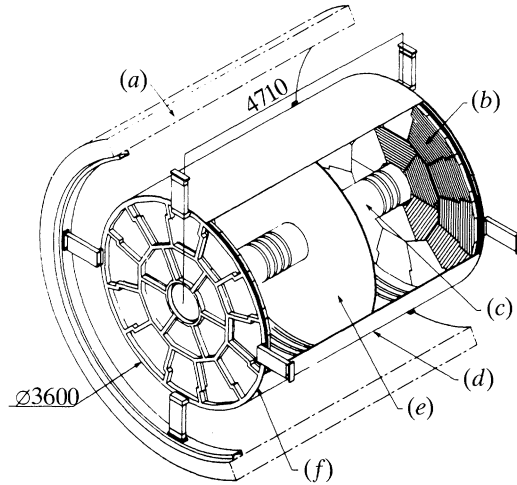
Figure 2. An isometric view of the ALEPH TPC. (*a*) Coil; (*b*) wire chambers; (*c*) inner field cage; (*d*) outer field cage; (*e*) HV membrane; (*f*) wire chamber support.

The coordinates are determined by a system of proportional wire chambers at the endplates with both anode wire and segmented cathode pad readout. There are 18 such chambers, referred to as sectors, on each endplate, as can be seen in figure 2. When the drifting electrons reach the vicinity of the anode wire an avalanche is formed causing a pulse on the anode and this induces a signal on typically two or three neighbouring cathode pads. Each endplate has a total of 20502 cathode pads arranged in 21 circular rows and 3168 sense wires situated on 6 inner and 12 outer sectors. The radial coordinate is that of the pad row, the azimuthal coordinate is determined from the relative pulse heights of neighbouring pad signals and the z coordinate from the drift time. The accuracy required demands the signals on all pads and wires be sampled at a high rate; 11.2 MHz is used so that for each event over 23 Mbytes of data are recorded. This involves major front end data reduction both in hardware and by 36 microprocessors so that the data transfer to the online system is *ca.* 50 kbytes.

Although the basic principle is simple and elegant much attention to detail is required for a TPC to produce data of the required accuracy. The main problems can be appreciated from examination of the formula for the drift velocity:

$$v_{\mathrm{d}} = \frac{\mu}{1+(\omega\tau)^2}\left(\boldsymbol{E} + (\omega\tau)\frac{\boldsymbol{E}\times\boldsymbol{B}}{|\boldsymbol{B}|} + (\omega\tau)^2\frac{(\boldsymbol{E}\cdot\boldsymbol{B})\,\boldsymbol{B}}{|\boldsymbol{B}|^2}\right)$$

with $\mu = e\tau/m$ the particle mobility, $\omega = eB/mc$ the cyclotron frequency, τ the mean time between collisions.

Ideally the electrons drift in straight lines parallel to the beam axis however from the above formula it can be seen that for this to take place the electric and magnetic fields must both be totally uniform, parallel to each other and parallel to the axis.

The effect of distortions depends upon the value of $\omega\tau$. Assuming the fields are almost parallel then $\boldsymbol{E}\times\boldsymbol{B}$ is small and so if $\omega\tau$ is significantly less than one the first term dominates and the electrons drift along the electric field lines whilst if $\omega\tau$ is significantly greater than one the third term dominates and the electrons drift along the magnetic field lines with only the direction determined by the electric field. In

ALEPH $\omega\tau \approx 9$ and therefore inhomogeneities in the magnetic field distort the electron trajectories while both these and electrical distortions lead to $\boldsymbol{E} \times \boldsymbol{B}$ problems.

Prevention of space charge build up – gating

Any non-uniformities in the electric field lead to $\boldsymbol{E} \times \boldsymbol{B}$ distortions. The cylinder walls of the TPC, which form the field cage, are constructed to very high precision; however, a major problem can be caused if there is any space charge build up within the drift volume. It is for this reason that the inner wall of the TPC is not too close to the beam where backgrounds can be high; the ITC is less sensitive. A serious cause of space charge distortions can, however, result from the avalanche processes in the proportional chambers at the endplates as these liberate positive ions which can drift into the main drift volume. These can cause severe and time variable distortions and must be eliminated by trapping the ions.

This is accomplished by a gating grid at the edge of the drift volume before the end chambers and makes use of the fact that $\omega\tau$ for the ions is much less than one and so, unlike the electrons, they follow the electric field lines. The gating voltage is removed just before the beams cross and reapplied shortly after if there is no positive trigger. Due to the low mobility of the ions they do not escape in the short time it is open and then, when it is closed, they follow the electric field lines of the gating grid to be captured at the grid electrodes.

Laser calibration

As the momentum is determined from the curvature in azimuth the critical distortions result from any ϕ-component of the drift velocity and this results primarily from the combination of small radial components in the magnetic field with the main component of the electric field in the $\boldsymbol{E} \times \boldsymbol{B}$ term. To evaluate the necessary corrections a sophisticated laser calibration system has been developed. Laser beams are transported from the top of the detector to splitter rings at the ends of the inner field cage of the TPC and from here the beams enter at three positions in azimuth and are reflected by a series of partly reflecting mirrors to provide five beams at different polar angles arranged so that they take the same trajectories as would particles with infinite momentum originating from the intersection point. The signals on the endplate wires are used to measure these trajectories; these give over 300 points per trajectory but have only information on the drift time or z coordinate. Nevertheless this information can be used to correct the azimuthal distortion which is the critical quantity for the momentum measurement. The laser tracks also enable the drift velocity and $\omega\tau$ to be measured.

Finally each sector of the TPC must be individually aligned to the ITC. This is achieved using the large sample of dimuon events which are now available and which provide two very clean tracks.

The effect of these procedures can be seen in figure 3 in which the inverse of the measured muon momentum from dimuon production $e^+e^- \rightarrow \mu^+\mu^-$ is plotted both before all these corrections in (*a*) and after in (*b*). Before correction the field distortions cause different mean values for the positive and negative muons but after correction this discrepancy is removed and the width of the peaks is significantly sharper. The result for the overall momentum resolution using both the TPC and ITC is

$$\Delta p/p = 0.0008p \quad (p \text{ in GeV}/c),$$

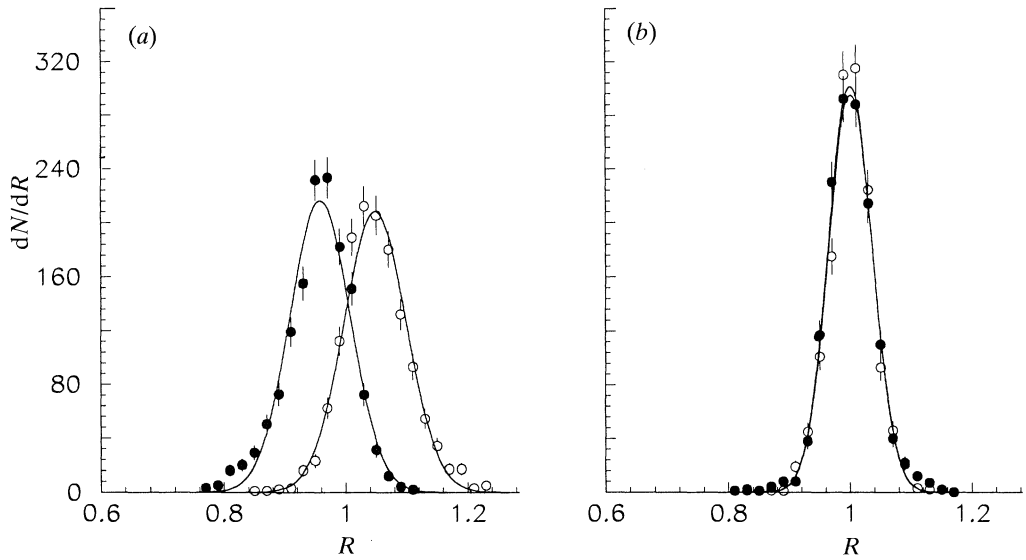which is very close to the original design value of $0.0007p$.

Figure 3. $R = E_{\mathrm{beam}}/p_{\mathrm{measured}}$ for the muons from $e^+e^- \to \mu^+\mu^-$ interactions (*a*) before corrections and (*b*) after corrections using measurements from both the ITC and TPC. ●, $Q = +1$; ○, $Q = -1$. (*b*) Momentum resolution: $\Delta p/p^2 = 0.0008\ \mathrm{GeV}^{-1}$.
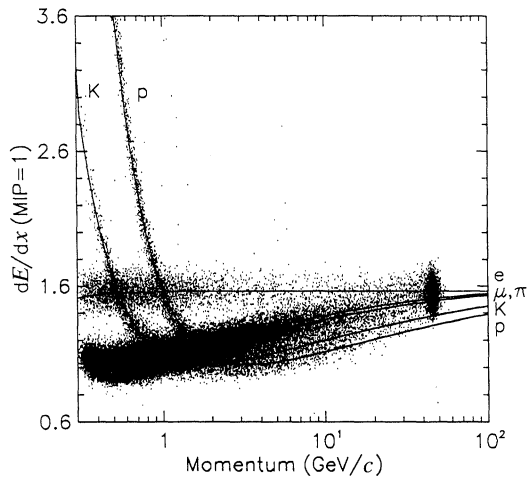

Figure 4. The measured $\mathrm{d}E/\mathrm{d}x$ from the TPC with expectations for the different particle types.

The corrections also enable accurate values of the impact parameter of the tracks at the origin to be measured. This has enabled ALEPH, with just the ITC and TPC, to measure the mean lifetime of the B states to a better accuracy than any previous measurement (Decamp *et al.* 1991). The value obtained is 1.29 ± 0.06 (stat) ± 0.10 (syst) ps to be compared with the previous world average value of 1.18 ± 0.11 ps.

dE/dx measurements

The pulse heights on the TPC wires enable the rate of loss of energy, dE/dx, to the gas of the TPC to be measured and this is used to distinguish particles of different types. The results are shown in figure 4 together with the theoretical expectation. The dE/dx error for a track with the maximum number of samples is *ca.* 5%.

4. Calorimetry

The emphasis for both the electromagnetic and hadronic calorimetry within ALEPH is on fine granularity with projective towers of the same size as the electromagnetic or hadronic showers. The fine granularity enables efficient identification of leptons in jets. It is also important for schemes to measure the total energy deposited from an interaction as it enables the contributions from charged tracks, which are more accurately measured with the tracking chambers, to be efficiently subtracted from the calorimetric deposits.

4.1. *The hadron calorimeter and muon identification*

The hadron calorimeter is a sandwich of iron and plastic streamer tubes. In total there is typically 1.2 m of iron providing more than seven interaction lengths for hadrons and embedded within this there are 23 planes of streamer tubes. Readout is via pads forming projective towers of $3.7° \times 3.7°$ and strips which give a one-dimensional digital signal for each tube. The pad signals give the energy measurement for the hadronic shower while the digital signals are used for muon identification by tracking the progress of the particles through the calorimeter. Muons are identified by their penetration abilities with the background from penetrating hadron showers removed by pattern-recognition algorithms on the digital signals. Muon chambers of the same construction as the streamer tube chambers within the calorimeter surround the iron. These have two-dimensional strip readout and add to the muon identification capability.

4.2. *The electromagnetic calorimeter and electron identification*

Very good identification of electrons in hadronic jets is one of the major strengths of ALEPH. The calorimeter was specifically designed for this. It is a highly granular lead-proportional tube sandwich with 74728 projective towers of approximately $0.8° \times 0.8°$. Each tower is readout in three stacks longitudinally; these have 4, 9 and 9 radiation lengths and are sampled 10, 22 and 13 times respectively. The calorimeter, when combined with the luminosity calorimeter, covers over 99% of the solid angle and in total there are nearly four million cathode pads. It has an essentially linear response to electrons and photons up to 50 GeV.

The large number of channels and the design goal of immediate data reconstruction have necessitated special techniques to provide real time correction for pedestal shifts from drifts in electronic components and gas amplification changes consequent on pressure or temperature variations. Pedestal drifts are corrected by following the calorimeter response during data-taking with an algorithm which updates the pedestals every few thousand triggers. Gas variations are tracked by a special proportional chamber, a platine, connected in the gas circuit for each module. This uses an Fe^{55} source to constantly monitor the gas amplification and produce corrections every hour for the front-end processors. As well as accounting for
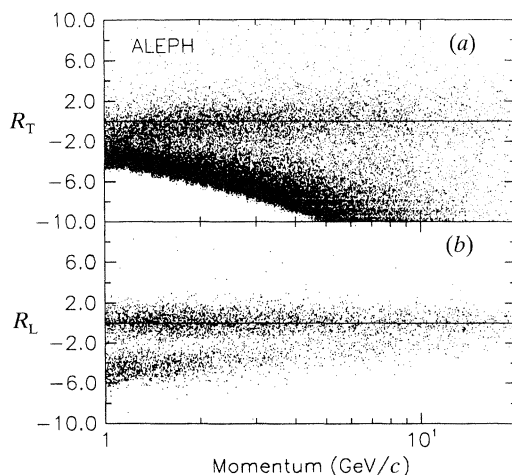
Figure 5. Electron discrimination variables against momentum (a) the value of R_T after a cut in R_L and (b) the value of R_I after cuts in R_T and R_L.

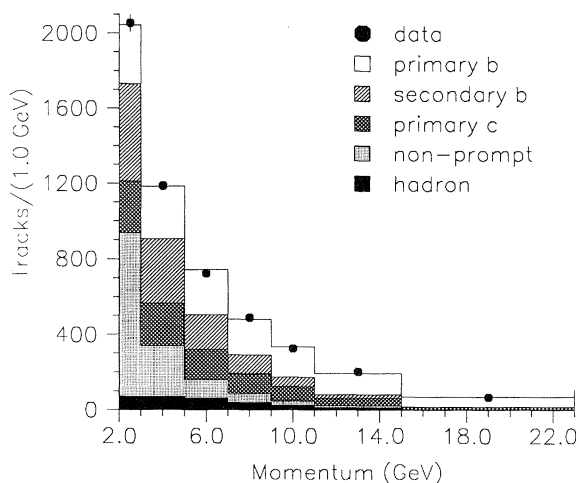

Figure 6. The inclusive electron momentum spectrum from hadronic decays of the Z showing the contributions from primary b decay (b→e), secondary b decay (b→c→e), primary c decay (c→e), non-prompt electrons (γ→e⁺e⁻), and hadron misidentification.

temperature and pressure variations the platines have also automatically provided the corrections for very small amounts of gas poisoning caused by faulty valves in a few of the modules. During the 1990 running this system held the gas amplification constant to better than 1 %.

To separate electrons from hadrons in the electromagnetic calorimeter the segmentation in both the transverse and longitudinal directions are used to define the shower profile. Two variables are defined which are normally distributed for electrons. One of these, R_T, depends on a comparison of track momentum with the energy deposited in the four towers closest to the track extrapolation and relates to the transverse compactness of the shower while the other, R_L, uses the three-fold longitudinal readout from the calorimeter to compare the shower development with
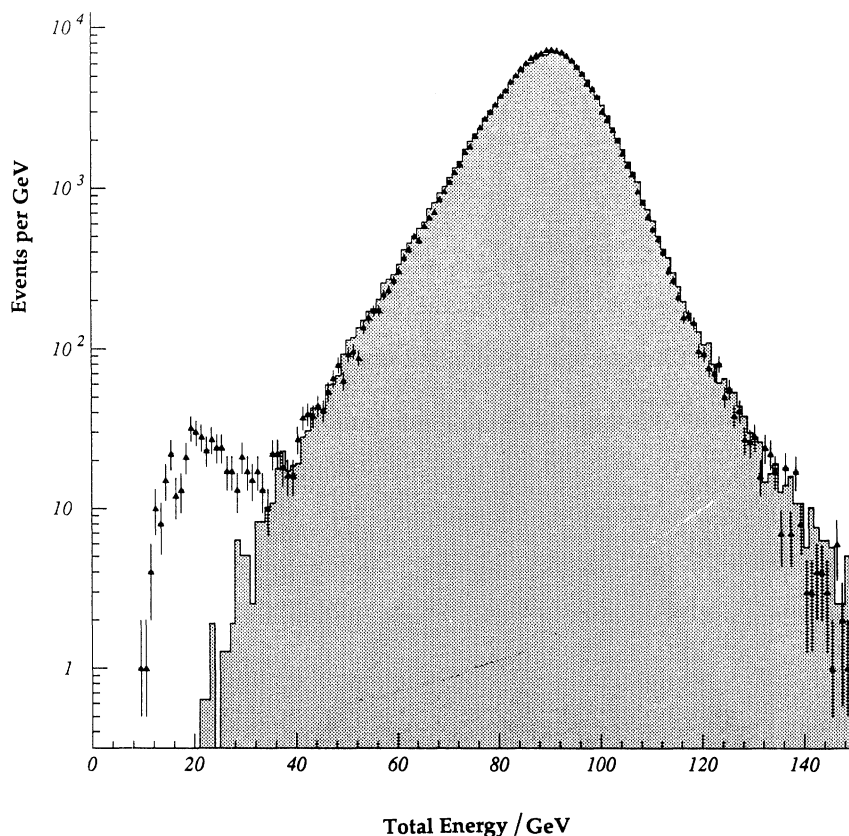
Figure 7. Comparison of the measured energy flow, data points, with that predicted from the Monte Carlo simulation, the shaded histogram, for hadronic decays of the Z.

that expected from an electron of that momentum. This separation is most efficient at high momentum; at low momentum it is improved by using the dE/dx measurements from the TPC and a third discrimination variable, R_I, normally distributed for electrons is defined on the basis of the observed dE/dx.

The combination of the two can be appreciated with the scatter plot of figure 5 which shows first the value of R_T against momentum for tracks which have passed the R_L cut and secondly the value of R_I against momentum for those tracks which pass both the calorimetric R_L and R_T cuts.

Hadron misidentification as electrons is very low and varies from 0.0004 per hadron to 0.003 as the momentum varies from 2 to 20 GeV. In figure 6 the measured momentum spectrum of electrons in hadronic events is shown together with the predictions for the origin of the electrons, b or c quark decays, external or internal photon conversions or the very small hadron misidentification background.

4.3. *Energy flow measurements*

Combination of the information from all tracking chambers and calorimeters enables the total energy emitted in an event and the direction of the energy flow for individual jets to be determined. The energy flow direction gives a much better measure of the direction of the original quark than the more commonly used mean

momentum vector of the charged tracks and hence provides a better axis for transverse momentum measurements which are used to generate a sample of clean b quark events. The measurements are also essential for efforts to either find the Higgs or put lower limits on its mass. In figure 7 the energy flow measurements are seen to agree well with Monte Carlo predictions over four decades and only fail when the energy observed in an event is sufficiently low that two photon events are included in the sample; these are absent in the Monte Carlo.

5. Luminosity measurement

The main luminosity monitor is of very similar construction to the main electromagnetic calorimeter. It also serves to complete the overall electromagnetic calorimetry as the petal structure used for the endcaps becomes very inefficient close to the beam line.

The performance of the luminosity monitor determines the error on the cross-section measurements. Although the choice of construction of the luminosity calorimeter results in a rather large inner radius and hence a low counting rate the calorimeter has a very high mechanical rigidity with the critical positions of the pads known with great accuracy. Consequently the systematic error, which is the critical one for the LEP cross sections is only 0.6% and expected to improve further.

6. Event reconstruction: FALCON

An early decision within ALEPH was that data should be reconstructed as soon as practicable and essentially online. This has two advantages; the physics tapes are quickly available to the collaboration for analysis and the reconstruction program provides a very powerful diagnostic for subtle faults which are not caught by the online checking procedures. Basic results from the reconstruction such as particle multiplicities, track fits, vertex positions, etc., are compared with those expected and this has proved very valuable for maintaining data quality.

The data reconstruction is achieved by the FALCON system, a local area cluster of 12 diskless VAX station 3100 CPUs controlled by a microVAX 3600. It is connected to the central online VAX 8700 via shared disks. Following each data taking run during which approximately 400 hadronic Z decays are produced the disk control is passed from the main machine to FALCON which then sends events to the processors where they are reconstructed in parallel. The reconstructed data with now *ca.* 25 kbytes of data per hadronic event are sent directly to the main CERN IBM and also to the ALEPH offline analysis VAX cluster on the CERN1 site. From the CERN computer centre the data is written to magnetic cartridges both for storage and for distribution to the participating institutes, usually within 24 h of data-taking.

The system has worked very well. Overall during 1989 and 1990 200 000 hadronic Z decays have been recorded by ALEPH corresponding to an integrated luminosity of *ca.* 8 pb^{-1}.

7. Future

It is planned that ALEPH will continue to take data at LEP for the full lifetime of the accelerator. No significant modification is required for running at the LEP2 energy.

For 1991 a new vertex detector will be introduced with two layers of double-sided

silicon detectors to that both ϕ and z coordinates can be measured. Physics resulting from vertexing will be further improved by use of the LEP beam observation monitors which will improve knowledge of the primary vertex. Also for 1991 a second layer of muon chambers has been added which will further decrease backgrounds to the muon sample.

If new schemes materialize to increase the number of bunches in LEP some changes will be necessary for the trigger and the readout of certain detectors. Little change is needed for an increase to eight bunches but substantial changes will be required if the possible change to 36 bunches occurs.

ALEPH is very keen to see an active polarization programme at LEP. For precision electroweak tests, with bunches in different polarization states, the low counting rate of the present luminosity calorimeter will become a limitation and consequently construction of a new silicon luminosity calorimeter is already underway. This will be closer to the beam and have a counting rate approximately four times greater than the present one while maintaining or improving the systematic error.

8. Summary

The ALEPH detector has enjoyed a highly successful first year and is well equipped to exploit the future programme of the LEP accelerator.

References

Decamp, D., *et al.* 1990 ALEPH Collaboration. ALEPH: a detector for electron–positron annihilations at LEP. *Nucl. Instrum. Methods Phys. Res.* A **294**, 121–178.

Decamp, D., *et al.* 1991 ALEPH Collaboration. Measurement of the B hadron lifetime. *CERN-PPE/90–195. Phys. Lett.* B **257**, 492–504.

8-2
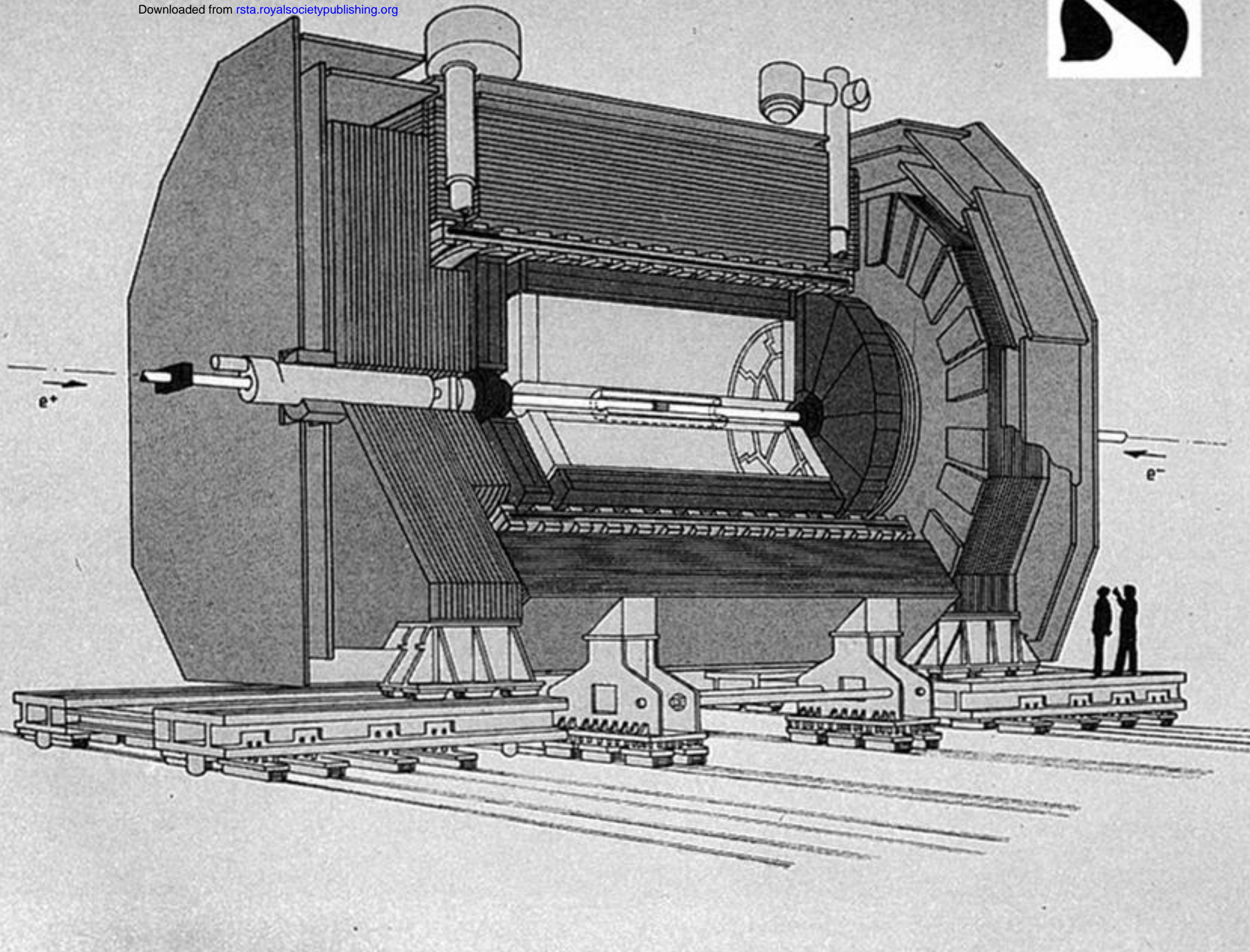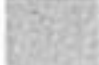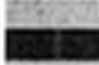
Vertex
Detector

Inner Track
Chamber

Time Projection
Chamber

Electromagnetic
Calorimeter

Superconducting
Magnet Coil

Hadron
Calorimeter

Muon Detection
Chambers

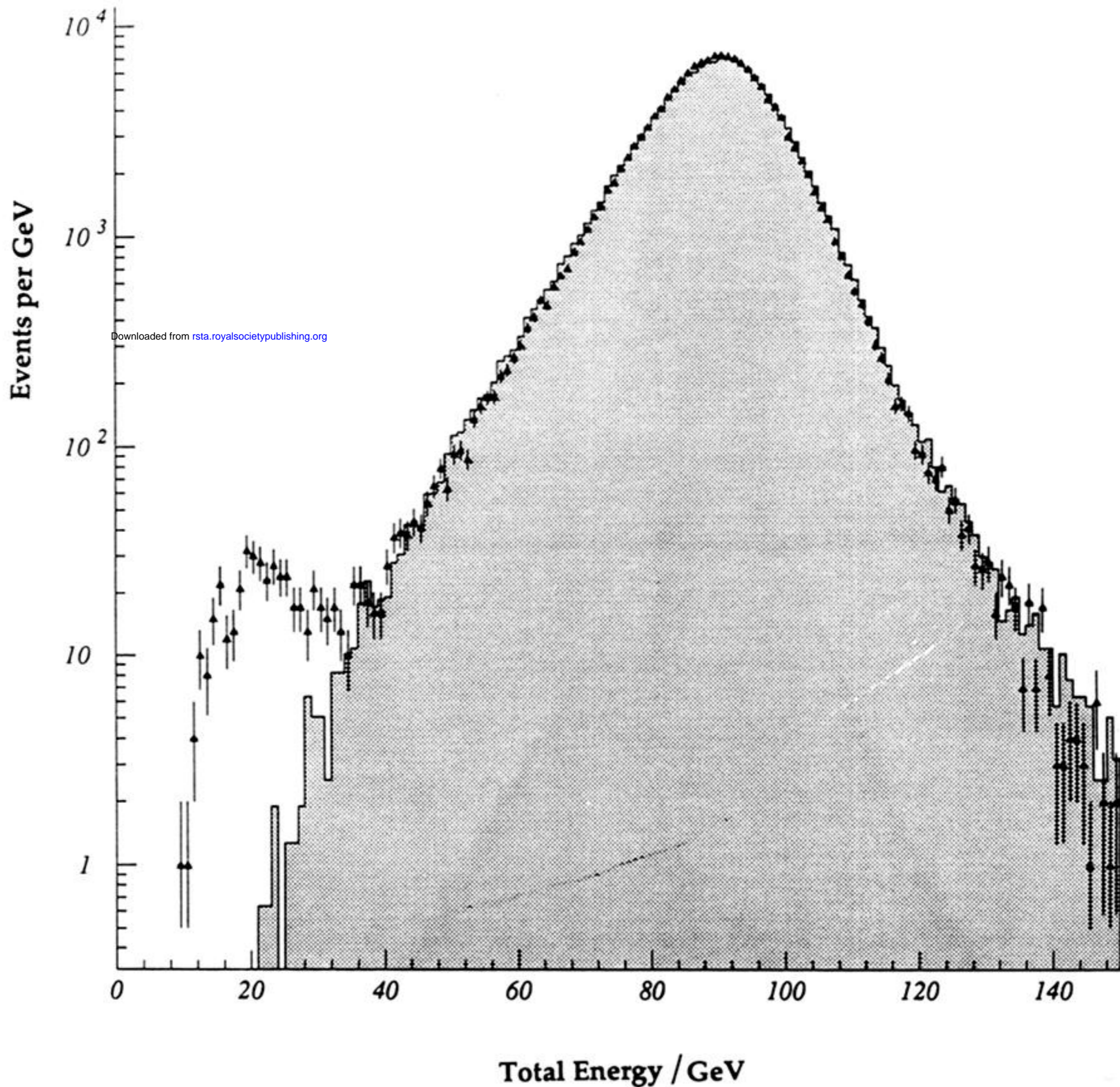Luminosity
Monitors

Figure 1. The ALEPH detector.

Figure 7. Comparison of the measured energy flow, data points, with that predicted from the Monte Carlo simulation, the shaded histogram, for hadronic decays of the Z.